



Published in final edited form as:

Semin Ultrasound CT MR. 2009 April ; 30(2): 91–104. doi:10.1053/j.sult.2008.12.002.

Image-guided thermal therapy of uterine fibroids

Shu-Huei Shen, MD^{1,2}, Fiona Fennessy, MD, PhD¹, Nathan McDannold, PhD¹, Ferenc Jolesz, MD¹, and Clare Tempany, MD¹

¹Department of Radiology, Brigham and Women's Hospital and Harvard Medical School, Boston, MA

²Department of Radiology, Taipei Veterans General Hospital and National Yang-Ming University School of Medicine, Taipei, Taiwan

Abstract

Thermal ablation is an established treatment for tumor. The merging of newly developed imaging techniques has allowed precise targeting and real-time thermal mapping. This article provides an overview of the image-guided thermal ablation techniques in the treatment of uterine fibroids. Background on uterine fibroids, including epidemiology, histology, symptoms, imaging findings and current treatment options, is first outlined. After describing the principle of magnetic resonance thermal imaging, we introduce the applications of image-guided thermal therapies, including laser ablation, radiofrequency ablation, cryotherapy and particularly the newest, magnetic resonance-guided focused ultrasound surgery, and how they apply to uterine fibroid treatment.

Introduction

Uterine fibroids are the most common benign neoplasm of the uterus. For women of childbearing age in the United States [1], they are the fifth gynecologic cause, unrelated to pregnancy, for hospitalizations. There are many treatment options available, and new approaches are under evaluation. The options range in degree of invasiveness from total uterine or fibroid removal, such as hysterectomy or myomectomy, to medical management or no treatment.

Surgery is a longstanding and well established treatment for uterine fibroids; however, advancements in medical technology have made less invasive treatment options available. One such option is image-guided thermal ablation, or the destruction of tissue by rapid temperature change. The development of image-based real-time “MR thermometry” methods, combined with anatomical imaging allows for a complete “closed loop” system for guided and monitored therapy. In this article, we outline the principles of various image-guided thermal therapies for fibroids including laser ablation, radiofrequency ablation (RFA), cryotherapy and focus particularly on magnetic resonance-guided focused ultrasound surgery (MRgFUS).

Correspondence to: Clare Tempany, MD, E-mail: ctempany@bwh.harvard.edu, Tel: +1 617-732-8772, Address: Department of Radiology, Brigham & Women's Hospital, 75 Francis St, Boston, MA 02115.

Institution: From the Departments of Radiology, Brigham and Women's Hospital and Harvard Medical School, 75 Francis St, Boston, MA 02115

Disclosure: Drs. Tempany, Jolesz and McDannold receive research support from InSightec Inc. Dr. Tempany is a consultant for InSightec. Dr. Jolesz is on the medical advisory board for InSightec.

Publisher's Disclaimer: This is a PDF file of an unedited manuscript that has been accepted for publication. As a service to our customers we are providing this early version of the manuscript. The manuscript will undergo copyediting, typesetting, and review of the resulting proof before it is published in its final citable form. Please note that during the production process errors may be discovered which could affect the content, and all legal disclaimers that apply to the journal pertain.

Uterine fibroids

Epidemiology/Histology

Uterine fibroids are benign clonal tumors of the smooth muscle cells [2]. Estimated incidence by 50 years of age is greater than 80% for black women and nearly 70% for white women [3]. Pathologically, they are smooth muscle neoplasms with some fibrous connective tissue. Histologically, they are nonencapsulated but demarcated from surrounding myometrium by a pseudocapsule of light areolar tissue or compressed myometrial tissue. They are categorized by their location in the uterus as intramural (entirely or mostly contained within the myometrium), submucosal (projecting into the endometrial cavity and may also be pedunculated), or subserosal (projecting outward from the serosal surface of uterus and may be pedunculated). Uterine fibroids are estrogen dependent and contain estrogen receptors, thus, they can enlarge during pregnancy or with the use of oral contraceptive pills and shrink after menopause. Fibroids can be subject to a wide variety of degenerative phenomena, especially during rapid growth including myxoid, hyaline, cystic, red (hemorrhagic), and fatty degeneration as well as calcification and necrosis. These all contribute to the complexity and variability of fibroid imaging appearance.

Symptoms

Approximately 25% of women with uterine fibroid have pelvic pain, menorrhagia, dysmenorrhagia, dyspareunia, pressure-related symptoms, such as pelvic fullness, and urinary frequency. They are thought to contribute to infertility and can be associated with early pregnancy losses and difficulty in maintaining a viable pregnancy. In general, the larger the fibroids, the more likely they are to be symptomatic; therefore, it is believed that by reducing fibroid size symptoms may improve [4]. Interestingly this does not always hold; even small fibroids, such as small submucosal ones that bleed a lot and can be very symptomatic.

Imaging: Ultrasound (US), computed tomography (CT) and magnetic resonance imaging (MRI)

US is usually the first imaging modality of choice for the detection and diagnosis of fibroids that typically appear as well-defined hypoechoic masses within the uterine wall. Subserosal fibroids may cause uterine enlargement and pedunculated ones may simulate an adnexal mass. Submucosal fibroids may cause distortion of the endometrial stripe. Fibroids are usually hypoechoic when small but may vary in imaging appearance as they grow and degeneration leads to further hypoechogenicity. They may contain calcifications or cystic spaces.

Given that CT has relatively poor soft tissue resolution, it plays a limited role in the diagnosis of uterine fibroids and their differentiation from other uterine pathologies such as adenomyosis and uterine malignancy. They appear as an enlarged uterus with or without calcifications, a deformed uterine contour, and uterine masses. CT's advantage in imaging uterine fibroids is its sensitivity in detecting internal calcification and hemorrhage.

MRI is the optimal imaging modality for diagnosing, characterizing, and localizing uterine fibroids due to its inherent soft tissue contrast resolution and a multiplanar capacity. A suggested MRI protocol for imaging and characterizing uterine fibroid is in Table 1. Typically, fibroids appear as a well-defined uterine mass with, compared to myometrium, a homogeneously low signal on a T2-weighted image that enhances after administration of IV gadolinium (Figure 1). By contrast, hypercellular fibroid, a variation of the uterine fibroid that is composed of compact smooth muscle cell without intervening collagen, usually shows a high signal intensity on T2-weighted imaging. That signal intensity represents fluid rich tissues that can enhance after IV Gadolinium contrast administration (Figure 2). When fibroids undergo a degenerative process, they may demonstrate a heterogeneous signal on both T1- and T2-weighted imaging

(Figure 3). Areas of calcification appear with very low signal intensity either clustered or rim-like. These features are more obvious on gradient echo T1-weighted images (Table 2).

MR is useful, particularly in differentiating pathologies such as adenomyosis, which may be similar clinically. Adenomyosis is typically an ill-defined myometrial “mass-like” lesion that manifests as widening of the transitional zone (>12 mm) without a capsule and usually with small hyperintense T2 spaces. Another entity that may be differentiated from fibroids is the rare possibility of leiomyosarcoma. However, while the presence of an irregular border and intrafibroid necrotic area with hemorrhage and variable signal intensity may appear suspicious, there are no strict imaging criteria to differentiate benign from malignant smooth muscle tumor so a diagnosis of leiomyosarcoma cannot always be made through imaging [5,6].

Treatment options for symptomatic fibroids

Medical management

Current medical treatment of uterine fibroids mainly involves hormonal manipulation. Gonadotrophin-releasing hormone (GnRH) analogues have been the most widely used for temporarily reducing fibroid size by as much as 30% to 60% and decreasing blood flow [7, 8]. Their use may influence the type of surgical approach (e.g. abdominal versus vaginal hysterectomy) and decrease blood loss during operation [9,10]. Similarly, GnRH antagonists can be used to induce a “medical menopause”. Compared to GnRH analogues, the onset of effects of the GnRH antagonists are faster. However, two major limitations are that symptoms are only controlled temporarily and will recur as soon as treatment is discontinued, and they are associated with side effects like tiredness, hot flashes, weight gain, and depression, all of which limit long-term use [2,11].

Surgical treatment

Hysterectomy has always been the ultimate way of resolving all fibroid-associated symptoms. In fact, the leading reason for hysterectomy in the United States has been uterine fibroids [12]. Studies of outcomes following hysterectomy indicate high patient satisfaction and improved quality of life. However, it is a major operation that has mortality rates in the range of 0.38–1 per 1000, severe complications in 3% of women, and minor in up to 30% women [13]. Long-term consequences, such as urinary incontinence and early ovarian failure, can occur or continue years after the operation.

For women with symptomatic fibroids desiring uterine conservation, their primary surgical treatment is myomectomy, the excision of a fibroid tumor from the uterus through laparoscopic or hysteroscopic approaches. Today, laparoscopic myomectomy is used frequently for intramural and subserosal fibroids and hysteroscopic myomectomy is used if the fibroid is submucosal [14]. Another advance in the field of laparoscopic surgery is the development of robotic-assisted laparoscopic surgery (RAS). By allowing the surgeon to be seated comfortably while visualizing the abdominal and pelvic cavities in a three-dimensional view, the procedure can be more precise and finely tuned than other methods [15]. Much of this experience incorporated the “da Vinci surgical system” that was approved in April 2005 by the Food and Drug Administration (FDA) for gynecologic applications [16]. However, due to recurrent symptoms, about one-fourth of women undergoing myomectomy will require further surgery [17].

Uterine artery embolization (UAE)

Uterine artery embolization (UAE) was first introduced in 1995 and involves femoral artery catheterization and intraarterial infusion of embolization particles, producing ischemia of the fibroid uterus and subsequently decreasing the volume of fibroids [18]. The procedure has

become widely accepted due to the advantage of its minimal invasiveness. All the large series comparing embolization with hysterectomy have favored embolization [19–24] in terms of its efficacy (80–90% symptom improvement for menorrhagia, pain and bulk-related symptoms) and rate of complications (1–4% major complications) [19–25]. Its major side effect is severe pain after the procedure [26–29]. Other complications include severe infection leading to hysterectomy (1.5%) and ovarian failure (5%) [21,28,29]. UAE has no known impact on fertility or miscarriage rates.

Image-guided thermal therapy

Introduction

Image-guided ablative therapy (IGT), encompassing the expertise in imaging technology and various tumor ablation techniques, is one of the most rapidly expanding fields in radiology and medicine. For many surgical procedures, it has been accepted as a less invasive alternative. In IGT, tumor ablation typically occurs when a clinician introduces it to a rapid thermal change ($> 55^{\circ}\text{C}$ for heat or $< -20\sim 50^{\circ}\text{C}$ for cold) [30]. To target the lesion for ablation and assess treatment response, the clinician uses imaging. Ideally, this imaging technique for guiding thermal ablation should provide target definition, anatomical information and temperature feedback. Recent developments in MR thermometry have made it the most reliable method for real-time temperature monitoring.

Magnetic resonance temperature imaging

The chemical environment and relaxation properties of nuclei are the source of the signal in MR. MR is also sensitive to Brownian motion and associated molecular tumbling rates; thus, MRI techniques are intrinsically sensitive to temperature. By choosing correct parameters, MR thermometry can provide all the requirements for thermal imaging during ablation, including temperature sensitivity, linearity of temperature effect, adequate spatial and temporal resolution, with minimal artifact [31–34]. Here we describe the most commonly used MR thermometry techniques.

The first parameter used for temperature imaging for therapeutic monitoring was the spin-lattice relaxation time (T_1) [35]. The primary mechanism for T_1 relaxation for water protons is the dipole-dipole interaction. T_1 's temperature dependence is very sensitive to temperature-dependent Brownian motion, and, thus, T_1 increases along with increasing temperature according to an approximately linear relationship. The method, relatively motion-insensitive, can be acquired rapidly. However, the parameter is highly tissue-dependent [36], and, therefore, the homogeneity of target tissue may affect the accuracy of thermal quantization. For example, as protein denaturation occurs [37], thermal temperature response becomes nonlinear. Therefore, the T_1 method is often only used to qualitatively measure temperature distribution during the rapid heat deposition ablation process.

Another parameter used for thermal mapping is the diffusion coefficient of the water molecule. Molecular water mobility due to Brownian motion is quantified by the diffusion coefficient that is temperature dependent [38], and, thus, can be used to measure temperature in vivo [39]. Its temperature sensitivity is high, but the acquisition times are too long. Further, it is extremely sensitive to motion. Another problem with the technique is that various physiological responses in tissue during the treatment, including edema, ischemia, cellular swelling and coagulation, can change local diffusion and interfere with temperature measuring.

So far, the proton resonance frequency (PRF) method is the most appropriate parameter for quantitative temperature monitoring. In this method, hydrogen bonds between local water molecules bend, stretch, and break as the temperature increases and the decreased net hydrogen bond strength results as the strength of the covalent bond between the water proton and its

oxygen increases. That effect better shields the proton from the external magnetic field and causes a proton resonance frequency (PRF) shift [40,41]. The PRF has an approximately linear relationship with the change in temperature [42] and, compared to the T1 relaxation time, very little tissue dependency. It has been shown that, except for adipose tissue, the PRF thermal coefficient is tissue type-independent and not much affected by tissue coagulation [43,44]. Although its acquisition time is relatively short as compared to the diffusion technique, PRF is sensitive to motion and to limit errors due to motion, several approaches have been investigated [45-47].

Laser ablation

The use of lasers for thermal therapy and local tumor necrosis was first described in 1983 [48]. Through a percutaneous approach, a laser fiber tip imbedded in tissue, infrared laser energy is converted to heat and causes a rise in temperature and eventual coagulative necrosis. The volume of necrosis created is proportional to the amount of laser power deposited in the tissue.

The laser ablation of fibroids was first described in 1989 as a procedure performed via the laparoscopic or endoscopic route [49]. It successfully decreased fibroid volume by 50% to 70% in symptomatic women via the hysteroscopic (submucosal fibroids) or the laparoscopic route (subserosal or intramural fibroids). In 1999, Law et al first reported percutaneous treatment of uterine fibroids by neodymium: yttrium-aluminium-garnet (Nd YAG) laser under MR guidance [50]. The treatment was monitored by MR thermometry using the T1 method whereby the operator places the laser tip accurately into the target fibroid to enable MR thermal monitoring with real-time feedback on temperature change and treatment area delineation. The loss of the T1 signal associated with temperature rise was converted into a color image that turned from blue to green as the temperature reached 55°C and irreversible tissue damage began to occur. In the mid-term follow-up series study [51], the reduction in mean fibroid volume was 31% at 3 months follow-up, and 41% at the one year follow-up.

Cryotherapy

Cryoablation is the thermal ablation method that causes cell death by rapid freezing followed by rapid thawing [52]. The temperature change causes cell membrane rupture and cellular dehydration as well as vascular stasis and thrombosis that lead to local tissue ischemia. The temperature must be lower than -20~50°C to completely destroy tissue. The cryoablation methods are based on the Joule-Thomson effect [53] so that by rapid expanding high-pressure argon gas within a cryoprobe a very low temperature results to create an ice ball. The computer-controlled gas distribution system also allows active thaw by helium gas.

Cryoablation for the uterine fibroid was initially introduced using either laparoscopic or hysteroscopic access [54-56]. In 2001, Sewell et al first reported its use for uterine fibroids with MR guidance [57]. Under MR imaging, the cryo lesion is very well visualized with a sharp very low SI on both T1- and T2-weighted imaging so the ice ball can be clearly delineated [58-61]. By monitoring the developing size of the ice ball and its relationship to the tumor, the clinician can control the process. Post-procedure complications include fever and abscess [62]. Prophylactic antibiotics administration is recommended. Follow-up studies showed variable results with volume reduction of fibroids ranging from 31% to about 80% [63,64].

Radiofrequency ablation (RFA)

Ablation of solid tumors with radiofrequency energy results from heating that is produced when ions follow the oscillations of a high-frequency alternating electric field [65]. The heat causes coagulation necrosis of local tissue. For more than 20 years, RFA has been accepted as a minimally invasive procedure for the local control of various malignant tumors. It was first

used in 2005 in the management of uterine fibroids via a surgical laparoscopic approach [66, 67] and subsequently with US guidance [68-70]. A large area of necrosis (up to 6 cm in diameter) can be achieved in a single access with RFA, and, therefore, compared to cryotherapy it is relatively time efficient. However, due to the incompatibility of RFA to MR [71], the currently used image guiding modalities for RFA are US or CT that, while good for lesion targeting, are unable to provide accurate temperature monitoring. The real ablation area could not be seen during the treatment, and thermal mapping is now possible. More recently, efforts to allow RF delivery under MR guidance have been made [72-74], although these are primarily used for liver ablations.

MR-guided focused US

Historical and technical development of MRgFUS

Focused US (FUS) is the therapeutic use of US waves to induce focal thermal effects, ablation, or thermocoagulation in vivo. The therapeutic use of FUS dates back to 1942 when Lynn et al first used it in the liver [75]. In the 1950s, the Fry brothers developed a complex FUS sonication system that used X-rays to determine the target location with respect to skull bones [76,77]. More recently, a combination of diagnostic US guidance and therapeutic high intensity focused US (HIFU) made soft tissue targeting and sonication possible. HIFU has been used extensively in different organs and diseases [78,79].

The acceptance of this ablation method in clinical practice, however, has been slow, particularly in the United States. One major factor in this delay is the inability using HIFU to clearly visualize the target lesion and monitor its ablation. This inability is overcome by the exciting development in the 1990s of MR-guided focused US surgery (MRgFUS). The initial device used a single element transducer in a high field MR magnet, to ablate focal tumors of rabbit muscle [80,81]. These experiments demonstrated the feasibility of using the focused US device within a MRI scanner, and more importantly, visualizing the focal heating and detecting the resulting tissue damage. Since the initial studies, substantial work has been done on developing MRI-compatible phased arrays and a driving system to increase the focal heating volume and steer the US beam. All components are designed to perform within the MR suite with a custom designed table.

As the technical and engineering research advanced, a new field of MR thermometry research and development began. The critical steps of testing and validating the MRI-based temperature methods have demonstrated the accuracy of the current methods. Using MR thermometry, it is possible to localize the focal spot and to monitor the ablated zone in real time.

The ExAblate 2000 (InSightec Inc., Haifa, Israel) is the first MRgFUS device approved by the FDA in 2004 for fibroid treatments. This device houses all of the electronics and the phased array transducer in a sealed water bath enclosed in a custom-built patient scanner table that docks to a 1.5T MR magnet (GEHC) (Figure 4). The ExAblate 2000 has been tested extensively in clinical trials for the treatment of uterine fibroids. Since then, the device has been adapted to allow treatment of other lesions such as the palliation of bone metastases, currently in clinical trials. This device has already been demonstrated for the treatment of breast fibroadenomas, breast cancer, and trials for brain tumor treatment and for liver diseases.

MRgFUS of uterine fibroids

Patient assessment and selection for MRgFUS

Patients with symptomatic fibroids referred for MRgFUS treatment should, as all patients, undergo a thorough clinical assessment evaluation, including history, physical exam (special attention to scar on the lower abdominal wall is important), and assessment of her clinical

symptoms. The latter can be objectively performed using a validated symptom severity questionnaire, a useful tool for establishing a baseline and for monitoring treatment response.

All women should also be screened for MR compatibility, as those who have contraindications to an MR examination, which include a cardiac pacemaker implantation, metallic implants such as Berry aneurysm clips, incompatible with MR, severe claustrophobia and pregnancy, are not eligible. The current FDA labeling indicates that the device should be limited to treatment of fibroids in women who are “family complete”.

As part of the initial evaluation, done at the time of the pre-treatment MRI, the woman should be able to lie prone on the MR table for about three hours and communicate sensation during the procedure. This is important to ensure a safe procedure. Scarring of the lower abdominal wall may disrupt the passage of the US waves through the skin and cause the US beam to become unfocused. If left unchecked, skin heating and burning can occur. Thus all prior surgeries, especially pelvic ones, must be visualized and documented.

At our hospital, all suitable subjects complete the symptom severity score (SSS) of Uterine Fibroid Symptoms and Quality of Life (UFS-QOL) Questionnaire [82], the only validated instrument for assessing symptoms specific for quality of life due to uterine fibroids. The SSS part is a 100-point scale composed of eight questions, assessing symptoms related to bleeding and bulk or volume-related complaints. The score is significantly higher in women with symptomatic fibroids who have a mean of 40, while normal women score approximately 20. These are objective measurements for pre-procedure evaluation and post-procedure monitoring.

Pre-procedure MRI

All eligible candidates for MRgFUS undergo a pre-procedure pelvic MR following a routine protocol using multiplanar T1- and T2- weighted imaging before and after IV gadolinium injection. This is best performed with the patient lying prone so that the images will closely resemble those on the day of treatment. This situation also gives the patient an opportunity to experience the prone treatment position before actually being scheduled for the procedure.

The MR is used to confirm the diagnosis of fibroids, rule out adenomyosis, and assess the fibroid number, size, location, tissue character and enhancement characteristics.

The imaging findings that need to be evaluated in pre-procedure MR and beam path planning are outlined in Table 3. Using the T2 images, the size of each fibroid is measured in three dimensions. Fibroids either too small (< 3 cm) or large (> 10 cm) are not suitable for treatment due to the inability to either target them or achieve enough necrosis. For large fibroids, pre-treatment with GnRH agonists allows shrinkage that shortens treatment times (Figure 5). Overall, by reducing vascularity, energy deposition can be potentiated. Thus, GnRH agonist treatment prior to MRgFUS will increase efficacy [10,83].

Procedure planning

There are several important issues to assess on the MR images. When preparing for MRgFUS, the path of US waves as they pass through tissue must be evaluated. If the target fibroid is too deep, the US may not penetrate deep enough. The upper limit is considered to be 12 cm from the anterior abdominal wall. If the fibroid is too close to the sacrum, the heating of the sacral bone may lead to sciatic nerve injury. It is best to limit the sonications to at least 4 cm from the sacral bone. All intervening or adjacent organs (bowel loops and urinary bladder) in the treatment path as well as the abdominal scar should be avoided.

The MR can determine the tissue composition and character of fibroids to allow for prediction of treatment response. As Lenard et al have shown the best candidate fibroids are those we call “classical”; these are low signal on all pulse sequences and enhance homogeneously with IV contrast [84]. Alternatively, the hypercellular ones, which have highly vascularized and fluid-rich tissue with high signal on T2-weighted images, are difficult to treat and therapeutic doses with normal FUS parameters may not be possible (Figure 6). They are associated with poor treatment effect and high failure rate [85-88]. However, if this is anticipated, treatment can be successful by adjusting factors such as increasing power. Also, if the fibroid is already degenerated and has a large necrotic area, MRgFUS is unlikely to improve symptoms. Additionally, an anterior calcification in the fibroids will cause interference with US propagation; therefore, it is a contraindication to treatment.

In summary, the ideal patient with fibroids for MRgFUS treatment is one with a fibroid located anteriorly, between 5 to 10 cm, and with a uniform low signal intensity on T2-weighted imaging, no intervening organ in the treatment pathway, and good perfusion without degeneration. To then ensure a successful treatment and high patient satisfaction, clinicians must effectively screen all candidates for treatment.

The MRgFUS procedure

Pre-procedure preparation

The procedure is performed with IV sedation, requiring the patient to fast the night before. The patients' abdomen will be cleaned and shaved from the umbilicus to 1 cm below the pubic bone.

The procedure is an outpatient one in an MR suite. On arrival, a nurse and MD assess the patient. An IV line is placed and urinary catheter will be positioned in the bladder to keep it empty during the course of the treatment. Conscious sedation, usually involving titrated doses of Fentanyl and Midazolam, along with monitoring of heart rate and pO₂, will be maintained for alleviating anxiety and relieving pain. The patient remains responsive through the whole procedure.

Treatment planning

Treatment is performed prone with the skin coupled to the FUS transducer with degassed water. Prior to the procedure, multiplanar T2-weighted images are acquired of the fibroid and uterus along with surrounding organs and abdominal wall. These images are then transferred to the ExAblate planning program. The region of treatment is manually drawn and defined within the capsule of the fibroid. The target volume is analyzed with superimposed US beam paths in all three planes (Figure 7). By angling the beam path (Figures 7 and 8), the target can be accessed optimally and avoid unwanted heating. When intervening bowel loops lie in beneath the abdominal wall, they can usually be displaced with external pressure using large gel pads or by distending the bladder (Figure 8).

Procedure

The procedure begins with the delivery of low-power sonication (50–100 W) to the center of the fibroid, with real-time thermometry acquired simultaneously through the PRF shift method. The resultant images provide feedback on sonication location to reconfirm targeting accuracy. Subsequent, sonications will be performed at a therapeutic power level to confirm thermometry (Figure 6). Energy delivered will be gradually increased until a therapeutic thermal dose is achieved to coagulate the entire volume of tissue at temperatures over 60° C. Between each sonication, adequate cooling time should be ensured to avoid thermal build-up and cause damage to normal tissues. The procedure continues with delivery of all planned sonications.

During the treatment, to ensure no complications occur, continuous communication with the patient is very important.

Typically the whole procedure (room time) takes 3-4 hours. Criteria to terminate the procedure early include the inability to visualize the focal treatment spot, patient complaints of unacceptable pain, and/or targeting difficulties due to patient motion or other reasons. After all sonications, the last step of the procedure is to assess the treatment effect by Gadolinium contrast-enhanced T1-weighted images. The resulting tissue necrosis appears as an area of non-enhancement in the fibroid (Figure 9). Before discharge, the MD examines the patient, looking at the skin surface for any possible heat-induced changes. The patient can be discharged home, on the same day usually 1-2 hours after the procedure, to be cared for by a responsible adult.

Summary of the literature

The initial phase I/II trial of the ExAblate 2000 device was conducted to evaluate the safety and feasibility of the new treatment. For this trial, premenopausal women with symptomatic fibroids (as defined by the SSS) were recruited. In this phase, they were all planning hysterectomy for their fibroids. The treatment protocol was limited to 100 mL of fibroid tissue, a 15 mm safety margin from both the serosal surface and the endometrium of the uterus, and 2 hours of sonication. As planned, a subsequent hysterectomy was performed within one month, allowing for direct pathological correlations.

Tempany et al reported the initial results of this trial, showing the safety and feasibility of the MRgFUS for treating uterine fibroids [89]. Through pathological correlation, the investigators demonstrated that MRgFUS could successfully cause thermal coagulation and necrosis in uterine fibroids. Most patients tolerated the procedure well without serious post- procedure consequence. After correlating the MR-treated volume and histological necrotic area, the pathologically documented necrosis was, interestingly, greater than the treatment volume [90]. Although there is no definite explanation, the coagulation of multiple blood vessels may be responsible for the phenomenon.

Subsequently, multicenter phase III clinical trials were carried out to evaluate the effectiveness and durability of the treatment. In this phase, after MRgFUS treatment, patients did not receive any additional forms of therapy. Enrollment criteria included, again, symptomatic fibroids and now they had to have no desire for further pregnancy or be “family complete”. The patients were followed and the outcome was assessed according to change in patient symptomatology as documented by the UFS-QOL Questionnaire scores at 6, 12, and now 24 months afterward and fibroid volume on MRI.

In the first short-term follow-up study by Hindley et al [91] in which 109 patients were recruited, 79.3% of treated women reported a significant improvement in their uterine fibroid symptoms. The mean reduction in fibroid volume at 6 months was 13.5%. In the study by Stewart, 71% of patients undergoing MRgFUS reached the targeted symptom reduction at 6 months, and 51% reached this point at 12 months [92]. Under the treatment with restriction protocol, on average, only less than 10% of the fibroid volume was sonicated. However, the result of treatment effect despite this very small volume was very encouraging. The results showed that, even with small volume reduction, symptom resolution can be achieved. This suggested that many of the symptoms were not related to the “bulk” or large size of the fibroids.

However there is no doubt reducing volume does indeed reduce symptoms. An important lesson from subsequent clinical trials is that the greater the treatment volume, the better the response achieved. After the safety of MRgFUS treatment was demonstrated, the FDA broadened the treatment guideline in 2004 to allow a treatment volume of 150 mL per fibroid with no restriction on the distance from the endometrium. Fennessy et al first analyzed the effect of the

different protocol on treatment results [93] and found that the relaxed treatment protocol resulted in a greater nonperfused volume, with 25.79% achieved versus the 16.65% of the restricted protocol ($P<.001$). For those treated with the restricted protocol, results of clinical follow-up showed that 74% of patients at 6 months, and 73% at 12 months had a greater than 10-point improvement in symptom score. In those treated, according to the relaxed protocol, 88% reported a 10-point or greater symptom improvement at 6 months, and 91% had significant symptom improvement at 12 months. The results proved that the less restrictive treatment protocol resulted in a larger treatment volume and better symptom improvement and durability. That conclusion was reconfirmed by looking into the subgroup of patients treated with the relaxed treatment protocol. Further analysis using a cut point of the 20% nonperfused volume ratio demonstrated that the nonperfused volume ratio had a very significant effect on the symptom severity score [94]. Compared to the low nonperfused volume ratio group, the high nonperfused volume ratio group had an average improvement of 6 points on the symptom severity score. Beyond 3 months, the high nonperfused volume ratio group maintained this improvement and had a slight increment of improvement that remained significant for up to 24 months.

Currently, MRgFUS has been broadly accepted as an option for the treatment of uterine fibroids. So far, more than 4000 patients have been treated with MRgFUS worldwide, with more than 3000 performed in routine clinical practice. In the recent reports of commercial treatment, with proper selection of patient population, the treatment volume is often more than 50%. The report of Mikami et al [86] showed the mean percent of nonperfused volume ratio in the 6-month follow-up was $47\% \pm 13\%$. Similarly, in the report by Morita et al [95], the mean percent of nonperfused volume ratio was 60% immediately upon completion of MRgFUS treatment, with the fibroids shrinking by about 39% at 6 months.

In summary, according to clinical outcomes studied so far, MRgFUS as an outpatient-based treatment is technically feasible, reproducible, and significantly reduces symptoms in more than 75% of women treated with fibroids. The rate of side effects is generally low. Transient adverse effects include mild skin burn, nausea, short-term buttock or leg pain, and transient sciatic nerve palsy [85-94]. Only one case of severe skin burn has been reported [96]. Another ongoing evaluation of the clinical application of MRgFUS is its impact on fertility. Rabinovici et al have reported on safe and successful outcomes of pregnancies after MRgFUS [97]. A new clinical trial is underway to evaluate the efficacy and safety of MRgFUS for the enhancement of fertility in women with uterine fibroids who are diagnosed with unexplained infertility [98-99].

Technical improvement

Strategies have been developed to increase the treatment volume and decrease treatment time. One of them is to use the so-called "interleave mode". By redefining the sonication order by minimizing overlap between sonications, less heat absorption in the pass zone can be achieved, and cooling time can be reduced to 22 seconds. Another effort is enhanced sonication. Different from the continuous power transmission that lasts about 20 seconds to gradually heat at the focus of the nominal sonications, the enhanced sonications are comprised of high power bursts followed by a period of no power. The high power generates microbubbles that cause energy reflection and greater energy absorption at the spot location. Therefore, although the total energy is the same, the volume of tissue ablated per individual sonication is much greater. Thus the treatment spot can be enlarged to allow for larger treatment volumes in shorter time periods. To determine the reliability and efficacy of enhanced sonication, a clinical trial have recently begun.

Technology assessment

Given the various treatment options for uterine fibroids, what is the relative position of MRgFUS in terms of long term outcome and cost? Like all new health care techniques, MRgFUS should be evaluated with respect to its ability to improve the patient's outcome and quality of life, and with regard to direct and indirect costs. General guidelines for technology assessment require careful review of all of the peer-reviewed literature and the scientific body of work.

Feasibility studies have proven the safety and efficacy of MRgFUS, an accomplishment that led to approval by the FDA. Multicenter clinical trials in large centers across the world have documented MRgFUS' efficacy in symptom reduction and resolution and its very low rate of side effects or adverse events. However, does the technology improve the net health outcome as much as, or more than, established alternatives? There has been no randomized controlled trials to date which have compared MRgFUS to other alternative treatment options of uterine fibroids. Decision modeling, providing a concise framework to quantify costs and outcomes, has been performed to estimate the cost effectiveness of MRgFUS in comparison to uterine artery embolization, myomectomy and hysterectomy [100]. This study concluded that a treatment strategy starting with MRgFUS was likely to be cost-effective. Thus as the data and published reports expand, it appears that MRgFUS will provide an excellent treatment option in appropriate women.

In summary, MRgFUS is still in evolution. Its potential applications are still being explored. Taking the great heterogeneity of technical access and availability in the real world into account, MRgFUS will likely be the single “best” treatment method in selected women. When approaching how to best treat uterine fibroids, a customized treatment strategy for each patient is still needed.

Acknowledgments

We would like to thank Kimberly Lawson for her help in preparing this article.

(1) NIH U41RR019703 (2) InSightec Inc. research clinical trial support

References

1. Velebil P, Wingo PA, Xia X, et al. Rate of hospitalization for gynecologic disorders among reproductive-age women in the United States. *Obstet Gynecol* 1995;86:764–769. [PubMed: 7566845]
2. Stewart EA. Uterine fibroids. *Lancet* 2001;357:293–298. [PubMed: 11214143]
3. Baird DD, Dunson DB, Hill MC, et al. High cumulative incidence of uterine leiomyoma in black and white women: ultrasound evidence. *Am J Obstet Gynecol* 2003;188:100–107. [PubMed: 12548202]
4. Pron G, Bennett J, Common A, et al. The Ontario Uterine Fibroid Embolization trial. Part 2. Uterine fibroid reduction and symptom relief after uterine artery embolization for fibroids. *Fertil Steril* 2003;79:120–127. [PubMed: 12524074]
5. Tanaka YO, Nishida M, Tsunoda H, et al. Smooth muscle tumors of uncertain malignant potential and leiomyosarcomas of the uterus: MR findings. *J Magn Reson Imaging* 2004;20:998–1007. [PubMed: 15558559]
6. Samuel A, Fennessy F, Tempany C, et al. Avoiding treatment of leiomyosarcomas: the role of magnetic resonance in focused ultrasound surgery. *Fertil Steril* 2008;90(3):850.e9–12. [PubMed: 18022163]
7. Weeks AD, Wilkinson N, Arora DS, et al. Menopausal changes in the myometrium: an investigation using a GnRH agonist model. *Int J Gynecol Pathol* 1999;18:226–232. [PubMed: 12090591]
8. Rutgers JL, Spong CY, Sinow R, et al. Leuprolide acetate treatment and myoma arterial size. *Obstet Gynecol* 1995;86:386–388. [PubMed: 7651647]

9. Crosignani PG, Vercellini P, Meschia M, et al. GnRH analogues before surgery for uterine leiomyomas. A review. *J Reprod Med* 1996;41:415–421. [PubMed: 8799917]
10. Lethaby A, Vollenhoven B, Sowter M. Efficacy of pre-operative gonadotrophin hormone releasing analogues for women with uterine fibroids undergoing hysterectomy or myomectomy: a systematic review. *BJOG* 2002;109:1097–108. [PubMed: 12387461]
11. Carlson KJ, Miller BA, Fowler FJ. The Maine Woman's Health Study II: Outcomes of the non-surgical management of leiomyomas, abnormal bleeding and chronic pelvic pain. *Obstet Gynecol* 1994b; 83:556–572. [PubMed: 8134066]
12. Farquhar CM, Steiner CA. Hysterectomy rates in the United States 1990–1997. *Obstet Gynecol* 2002;99:229–234. [PubMed: 11814502]
13. Banu NS, Manyonda I. Alternative medical and surgical options to hysterectomy. *Best Pract Res Clin Obstet Gynaecol* 2005;19:431–449. [PubMed: 15985257]
14. Falcone T, Bedaiwy MA. Minimally invasive management of uterine fibroids. *Curr Opin Obstet Gynecol* 2002;14:401–407. [PubMed: 12151830]
15. Advincula AP, Xu X, Goudeau S 4th, et al. Robot-assisted laparoscopic myomectomy versus abdominal myomectomy: a comparison of short-term surgical outcomes and immediate costs. *J minim invasive gynecol* 2007;14(6):698–705. [PubMed: 17980329]
16. Advincula AP, Song A. The role of robotic surgery in gynecology. *Curr Opin Obstet Gynecol* 2007;19 (4):331–336. [PubMed: 17625414]
17. Candiani GB, Fedele L, Parazzini F. Risk of recurrence after myomectomy. *Br J Obstet Gynaecol* 1991;98:385–389. [PubMed: 2031897]
18. Ravina J, Herbretreau D, Ciraru-Vigner N, et al. Arterial embolisation to treat uterine myomata. *Lancet* 1995;346:671–672. [PubMed: 7544859]
19. Walker WJ, Pelage JP. Uterine artery embolization for symptomatic fibroids: Clinical results in 400 women with imaging follow up. *Br J Obstet Gynaecol* 2002;109:1262–1272.
20. Pron G, Bennett J, Common A, et al. The Ontario uterine fibroid embolization trial: Uterine fibroid reduction and symptom relief after uterine artery embolization for fibroids. *Fertil Steril* 2003;79:120–127. [PubMed: 12524074]
21. Pinto I, Chimeno P, Romo A, et al. Uterine fibroids: Uterine artery embolization versus abdominal hysterectomy for treatment. A prospective, randomized, and controlled clinical trial. *Radiology* 2003;226:425–531. [PubMed: 12563136]
22. Spies JB, Cooper JM, Worthington-Kirsch R, et al. Outcome of uterine embolization and hysterectomy for leiomyomas: Results of a multicenter study. *Am J Obstet Gynecol* 2004;191:22–31. [PubMed: 15295340]
23. Spies JB, Spector A, Roth AR, et al. Complications of uterine artery embolization for leiomyomata. *Obstet Gynecol* 2002;100:873–880. [PubMed: 12423844]
24. Pron G, Mocarski E, Cohen M, et al. Hysterectomy for complications after uterine artery embolization for leiomyoma: Results of a Canadian multicenter clinical trial. *J Am Assoc Gynecol Laparosc* 2003;10:99–106. [PubMed: 12555002]
25. Hirst A, Dutton S, Wu O, et al. A multi-centre retrospective cohort study comparing the efficacy, safety and cost-effectiveness of hysterectomy and uterine artery embolisation for the treatment of symptomatic uterine fibroids. The HOPEFUL study. *Health Technol Assess* 2008;12(5):1–248. [PubMed: 18331704]
26. Goodwin S, Walker W. Uterine artery embolisation for the treatment of uterine fibroids. *Curr Opin Obstet Gynaecol* 1998;10:315–320.
27. Worthington-Kirsch RL, Popky GL, Hutchins FL. Uterine arterial embolization for leiomyomas: Quality-of-life assessment and clinical response. *Radiology* 1998;208:625–629. [PubMed: 9722838]
28. Roth AR, Spies JB, Walsh S, et al. Pain after uterine fibroid embolization for leiomyomata: Can its severity be predicted and dose the severity predict outcome? *J Vasc Interv Radiol* 2000;11:1047–1052. [PubMed: 10997469]
29. Spies JB, Roth A, Jha RC, et al. Leiomyomata treated with uterine fibroid embolization: Factors associated with successful symptom and imaging outcome. *Radiology* 2002;222:45–52. [PubMed: 11756703]

30. Jolesz FA, Silverman SG. Interventional magnetic resonance therapy. *Semin Interv Radiol* 1995;12:20–27.
31. Chung AH, Jolesz FA, Hynynen K. Thermal dosimetry of a focused ultrasound beam in vivo by magnetic resonance imaging. *Med Phys* 1999;26(9):2017–26. [PubMed: 10505893]
32. Pisani LJ, Ross AB, Diederich CJ, et al. Effects of spatial and temporal resolution for MR image-guided thermal ablation of prostate with transurethral ultrasound. *J Magn Reson Imaging* 2005;22:109–118. [PubMed: 15971190]
33. Quesson B, de Zwart JA, Moonen CT. Magnetic resonance temperature imaging for guidance of thermotherapy. *J Magn Reson Imaging* 2000;12:525–533. [PubMed: 11042633]
34. Rieke V, Pauly KB. MR Thermometry. *J Magn Reson Imaging* 2008;27:376–390. [PubMed: 18219673]
35. Philips D. Laparoscopic leiomyoma coagulation (myolysis). *Gynaecol Endosc* 1995;4:5–11.
36. Young IR, Hand JW, Oatridge A, et al. Modeling and observation of temperature changes in vivo using MRI. *Magn Reson Med* 1994;32:358–369. [PubMed: 7984068]
37. Nelson TR, Tung SM. Temperature dependence of proton relaxation times in vitro. *Magn Reson Imaging* 1987;5:189–199. [PubMed: 3041151]
38. Simpson JH, Carr HY. Diffusion and nuclear spin relaxation in water. *Phys Rev* 1958;111:1201–2.
39. Bleier AR, Jolesz FA, Cohen MS, et al. Real-time magnetic resonance imaging of laser heat deposition in tissue. *Magn Reson Med* 1991;21:132–137. [PubMed: 1943670]
40. Hindman JC. Proton resonance shift of water in the gas and liquid states. *J Chem Phys* 1966;44(12):4582–4592.
41. McDannold N. Quantitative MRI-based temperature mapping based on the proton resonant frequency shift: review of validation studies. *Int J Hyperthermia* 2005;21:533–546. [PubMed: 16147438]
42. Hoffman MM, Conradi MS. Are there hydrogen bonds in supercritical water? *J Am Chem Soc* 1997;119:3811–3817.
43. Peters RD, Hinks RS, Henkelman RM. Ex vivo tissue-type independence in proton-resonance frequency shift MR thermometry. *Magn Reson Med* 1998;40:454–459. [PubMed: 9727949]
44. Kuroda K, Oshio K, Mulkern RV, et al. Optimization of chemical shift selective suppression of fat. *Magn Reson Med* 1998;40:505–510. [PubMed: 9771566]
45. de Senneville BD, Quesson B, Moonen CT. Magnetic resonance temperature imaging. *Int J Hyperthermia* 2005;21(6):515–531.
46. Paliwal V, El-Sharkawy AM, Du X, et al. SSFP-based MR thermometry. *Magn Reson Med* 2004;52(4):704–708. [PubMed: 15389940]
47. Scheffler K. Fast frequency mapping with balanced SSFP: theory and application to proton-resonance frequency shift thermometry. *Magn Reson Med* 2004;51(6):1205–1211. [PubMed: 15170841]
48. Bown S. Phototherapy of tumours. *World J Surg* 1983;7:700–709. [PubMed: 6419477]
49. Nisolle M, Smets M, et al. Laparoscopic myolysis with the neodymium-Yttrium Aluminium Garnet Laser. *J Gynaecol Surg* 1993;9:95–99.
50. Law PA, Gedroyc WM, Regan L. Magnetic resonance guided percutaneous laser ablation of uterine fibroids. *Lancet* 1999;354:2049–2050. [PubMed: 10636374]
51. Hindley JT, Law PA, Hickey M, et al. Clinical outcomes following percutaneous magnetic resonance image guided laser ablation of symptomatic uterine fibroids. *Human Reproduction* 2002;17(10):2737–2741. [PubMed: 12351555]
52. Rubinsky B, Lee CY, Bastacky J, et al. The process of freezing and the mechanism of damage during hepatic cryosurgery. *Cryobiology* 1990;27:85–97. [PubMed: 2311412]
53. Hewitt PM, Zhao J, Akhter J, et al. A comparative laboratory study of liquid nitrogen and argon gas cryosurgery systems. *Cryobiology* 1997;35:303–308. [PubMed: 9425653]
54. Olive DL, Rutherford T, Zreik T, et al. Cryomyolysis in the conservative treatment of uterine fibroids. *J Am Assoc Gynecol Laparosc* 1996;3(suppl):S36.
55. Zreik TG, Rutherford TJ, Palter SF, et al. Cryomyolysis, a new procedure for the conservative treatment of uterine fibroids. *J Am Assoc Gynecol Laparosc* 1998;5:33–38. [PubMed: 9454874]

56. Zupi E, Piredda A, Marconi D, et al. Directed laparoscopic cryomyolysis: a possible alternative to myomectomy and/or hysterectomy for symptomatic leiomyomas. *Am J Obstet Gynecol* 2004;190:639–643. [PubMed: 15041993]
57. Sewell PE, Arriola RM, Robinette L, et al. Real-time IMR-imaging-guided cryoablation of uterine fibroids. *J Vasc Interv Radiol* 2001;12:891–893.
58. Silverman SG, Tuncali K, Adams DF, et al. MR imaging-guided percutaneous cryotherapy of liver tumors: initial experience. *Radiology* 2000;217:657–664. [PubMed: 11110925]
59. Matsumoto R, Oshio K, Jolesz FA. Monitoring of laser and freezing-induced ablation in the liver with T1-weighted MR imaging. *J Magn Reson Imaging* 1992;2:555–562. [PubMed: 1392248]
60. Matsumoto R, Selig AM, Colucci VM, et al. MR monitoring during cryotherapy in the liver: predictability of histologic outcome. *J Magn Reson Imaging* 1993;3:770–776. [PubMed: 8400564]
61. Pease GR, Wong ST, Roos MS, et al. MR image-guided control of cryosurgery. *J Magn Reson Imaging* 1995;5:753–760. [PubMed: 8748498]
62. Sakuhara Y, Shimizu T, Kodama Y, et al. Magnetic Resonance-Guided Percutaneous Cryoablation of Uterine Fibroids: Early Clinical Experiences. *Cardiovasc Intervent Radiol* 2006;29:552–555. [PubMed: 16532267]
63. Cowan BD. Myomectomy and MRI-directed cryotherapy. *Semin Reprod Med* 2004;22(2):143–148. [PubMed: 15164309]
64. Sakuhara Y, Shimizu T, Kodama Y, et al. Magnetic resonance-guided percutaneous cryoablation of uterine fibroids: early clinical experiences. *Cardiovasc Intervent Radiol* 2006;29(4):552–558. [PubMed: 16532267]
65. Organ LW. Electrophysiologic principles of radiofrequency lesion making. *Appl Neurophysiol* 1976;39:69–76. [PubMed: 1052287]
66. Bergamini V, Ghezzi F, Cromi A, et al. Laparoscopic radiofrequency thermal ablation: a new approach to symptomatic uterine myomas. *Am J Obstet Gynecol* 2005;192:768–773. [PubMed: 15746670]
67. Milic A, Asch MR, Hawrylyshyn PA, et al. Laparoscopic ultrasound-guided radiofrequency ablation of uterine fibroids. *Cardiovasc Intervent Radiol* 2006;29:694–698. [PubMed: 16502165]
68. Kim HS, Tsai J, Jacobs MA, et al. Percutaneous image-guided radiofrequency thermal ablation for large symptomatic uterine leiomyomata after uterine artery embolization: a feasibility and safety study. *J Vasc Interv Radiol* 2007;18:41–48. [PubMed: 17296703]
69. Recaldini C, Carrafiello G, Lagana D, et al. Percutaneous Sonographically Guided Radiofrequency Ablation of Medium-Sized Fibroids: Feasibility Study. *AJR Am J Roentgenol* 2007;189:1303–1306. [PubMed: 18029862]
70. Cho HH, Kim JH, Kim MR. Transvaginal radiofrequency thermal ablation: A day-care approach to symptomatic uterine myomas. *Australian and New Zealand Journal of Obstetrics and Gynaecology* 2008;48:296–301. [PubMed: 18532962]
71. Vigen KK, Jarrard J, Rieke V, et al. In vivo porcine liver radiofrequency ablation with simultaneous MR temperature imaging. *J Magn Reson Imaging* 2006;23:578–584. [PubMed: 16508928]
72. Zhang Q, Chung YC, Lewin JS, et al. A method for simultaneous RF ablation and MRI. *J Magn Reson Imaging* 1998;8:110–114. [PubMed: 9500269]
73. Botnar RM, Steiner P, Dubno B, et al. Temperature quantification using the proton frequency shift technique: in vitro and in vivo validation in an open 0.5 Tesla interventional MR scanner during RF ablation. *J Magn Reson Imaging* 2001;13:437–444. [PubMed: 11241819]
74. Clasen S, Pereira PL. Magnetic Resonance Guidance for Radiofrequency Ablation of Liver Tumors. *J Magn Reson Imaging* 2008;27:421–433. [PubMed: 18219677]
75. Lynn JG, Zwemer RL, et al. A new method for the generation and use of focused ultrasound in experimental biology. *J Gen Physiol* 1942;26:179–193.
76. Fry WJ, Barnard JW, Fry EJ, et al. Ultrasonic lesions in the mammalian central nervous system. *Science* 1995;122:517–518. [PubMed: 13255886]
77. Fry WJ, Fry FJ. Fundamental neurological research and human neurosurgery using intense ultrasound. *IRE Trans Med Electron* 1960;ME-7:166–181. [PubMed: 13702332]
78. Kennedy JE. High-intensity focused ultrasound in the treatment of solid tumours. *Nat Rev Cancer* 2005;5(4):321–327. [PubMed: 15776004]

79. Dubinsky TJ, Cuevas C, Dighe MK, et al. High-intensity focused ultrasound: current potential and oncologic applications. *AJR Am J Roentgenol* 2008;190(1):191–199. [PubMed: 18094311]
80. Cline HE, Schenck JF, Hynynen K, et al. MR-guided focused ultrasound surgery. *J Comput Assist Tomogr* 1992;16:956–965. [PubMed: 1430448]
81. Hynynen K, Darkazanli A, Unger E, et al. MRI-guided noninvasive ultrasound surgery. *Med Phys* 1993;20:107–115. [PubMed: 8455489]
82. Spies JB, Coyne K, Guaou Guaou N, et al. The UFS-QOL, a new disease-specific symptom and health-related Quality of Life Questionnaire for leiomyomata. *Obstet Gynecol* 2002;99(2):290–300. [PubMed: 11814511]
83. Smart OC, Hindley JT, Regan L, et al. Gonadotrophin-releasing hormone and magnetic-resonance-guided ultrasound surgery for uterine leiomyomata. *Obstetrics & Gynecology* 2006;108(1):49–54. [PubMed: 16816055]
84. Lénárd ZM, McDannold NJ, Fennessy FM, et al. Uterine Leiomyomas: MR Imaging-guided Focused Ultrasound Surgery—Imaging Predictors of Success. *Radiology* 2008;249:187–194. [PubMed: 18695211]
85. Ueda H, Togashi K, Konishi I, et al. Unusual appearances of uterine leiomyomas: MR imaging findings and their histopathologic backgrounds. *Radiographics* 1999;19:131–145.
86. Mikami K, Murakami T, Okada A, et al. Magnetic resonance imaging-guided focused ultrasound ablation of uterine fibroids: early clinical experience. *Radiat Med* 2008;26:198–205. [PubMed: 18509719]
87. Funaki K, Fukunishi H, Funaki T, et al. Magnetic resonance-guided focused ultrasound surgery for uterine fibroids: Relationship between the therapeutic effects and signal intensity of preexisting T2-weighted magnetic resonance images. *Am J Obstet Gynecol* 2007;196:184.e1–184.e6. [PubMed: 17306674]
88. Funaki K, Sawada K, Maeda F, et al. Subjective effect of magnetic resonance-guided focused ultrasound surgery for uterine fibroids. *J Obstet Gynaecol Res* 2007;33(6):834–839. [PubMed: 18001451]
89. Tempany CM, Stewart EA, McDannold N, et al. MR imaging guided focused ultrasound surgery of uterine leiomyomas: a feasibility study. *Radiology* 2003;226:897–905. [PubMed: 12616023]
90. Stewart EA, Gedroyc WM, Tempany CM, et al. Focused ultrasound treatment of uterine fibroid tumors: safety and feasibility of a noninvasive thermoablative technique. *Am J Obstet Gynecol* 2003;189:48–54. [PubMed: 12861137]
91. Hindley J, Gedroyc W, Regan L, et al. MRI guidance of focused ultrasound therapy of uterine fibroids: early results. *AJR Am J Roentgenol* 2004;183:1713–1719. [PubMed: 15547216]
92. Stewart EA, Rabinovici J, Tempany CM, et al. Clinical outcomes of focused ultrasound surgery for the treatment of uterine fibroids. *Fertil Steril* 2006;85:22–29. [PubMed: 16412721]
93. Fennessy F, Tempany CM, McDannold N, et al. MRI-guided focused ultrasound surgery of uterine leiomyomas: results of different treatment guideline protocols. *Radiology* 2007;243:885–893. [PubMed: 17446521]
94. Stewart EA, Gostout B, Rabinovici J, et al. Sustained Relief of Leiomyoma Symptoms by Using Focused Ultrasound Surgery. *Obstetrics and Gynecology* 2007;110(2):279–287. [PubMed: 17666601]
95. Morita Y, Ito N, Hikida H. Non-invasive magnetic resonance imaging-guided focused ultrasound treatment for uterine fibroids – early experience. *Eur J Obstet Gynecol Reprod Biol* 2008;139(2):199–203. [PubMed: 18160200]
96. Leon-Villapalos J, Kaniorou-Larai M, Dziewulski P, et al. Full thickness abdominal burn following magnetic resonance guided focused ultrasound therapy. *Burns* 2005;31:1054–1055. [PubMed: 15970389]
97. Rabinovici J, David M, Fukunishi M, et al. MR guided focused ultrasound pregnancies: pregnancy outcome following magnetic resonance guided focused ultrasound surgery (MRgFUS) for conservative treatment of uterine fibroids. *Fertil Steril*. in press
98. Morita Y, Ito N, Ohashi H, et al. Pregnancy following MR-guided focused ultrasound surgery for a uterine fibroid. *Int J Gynaecol Obstet* 2007;99(1):56–57. [PubMed: 17599842]

99. Gavrilova-Jordan LP, Rose CH, Traynor KD, et al. Successful term pregnancy following MR-guided focused ultrasound treatment of uterine leiomyoma. *J Perinatol* 2007;27(1):59–61. [PubMed: 17180132]
100. Zowall H, Cairns JA, Brewer C, et al. Cost-effectiveness of magnetic resonance-guided focused ultrasound surgery for the treatment of uterine fibroids. *BJOG* 2008;115:653–662. [PubMed: 18333948]

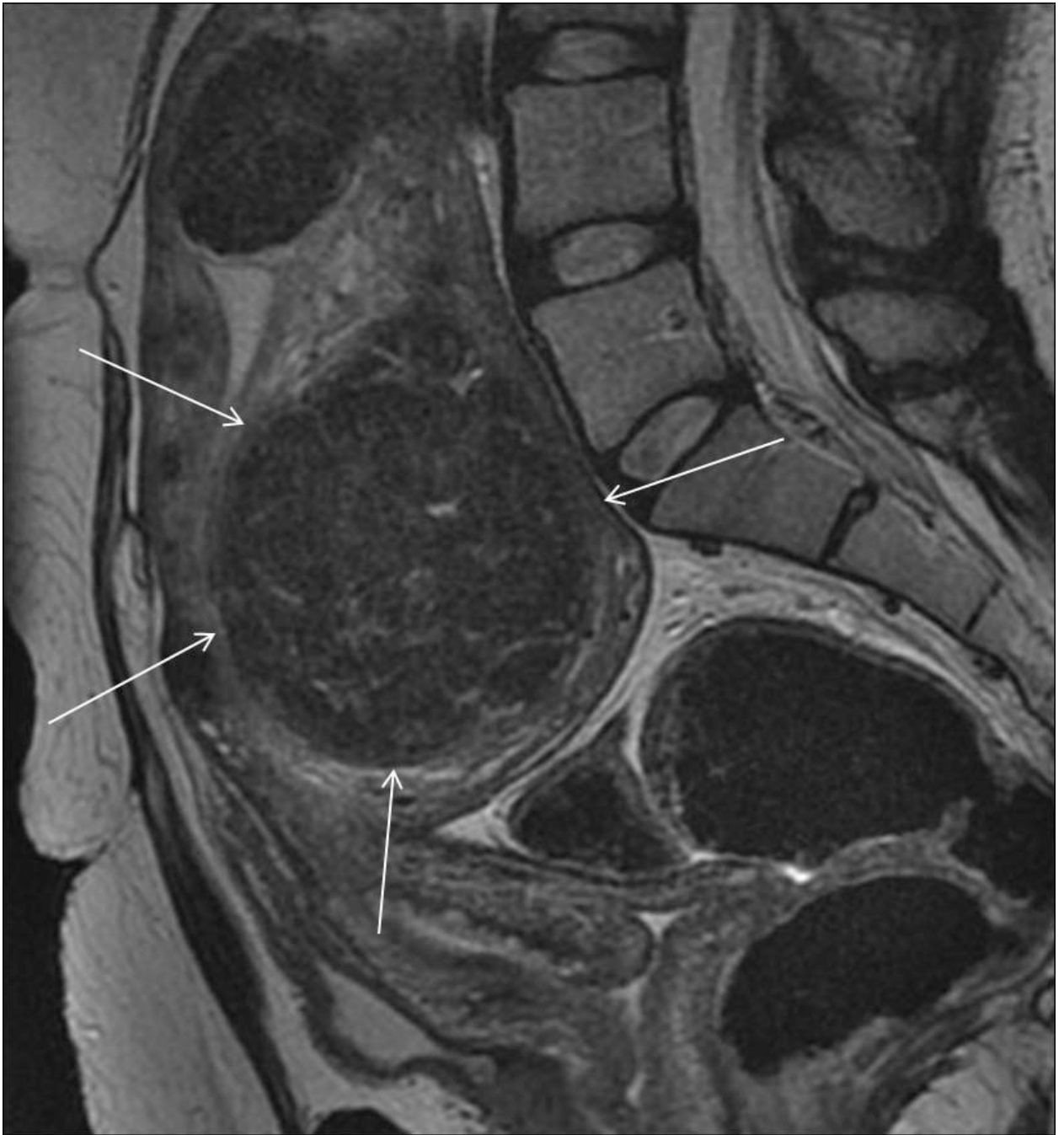


Figure 1. Classic uterine fibroid. On T2 weighted sagittal MR imaging, uterine fibroid (arrows) shows characteristic homogeneously low signal intensity.

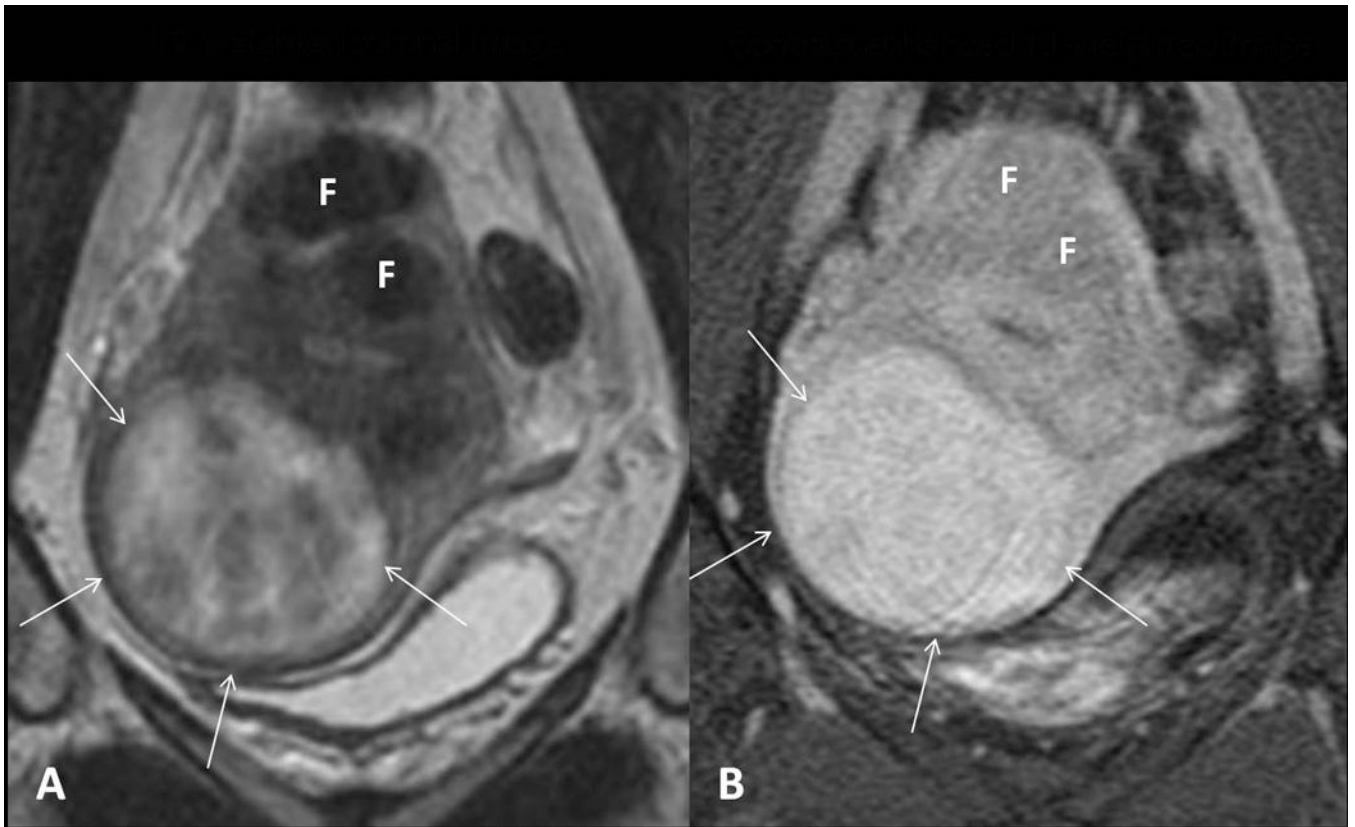


Figure 2. Hypercellular uterine fibroid. (A) On T2 weighted coronal MR imaging, the hypercellular fibroid (arrows) shows high signal intensity as compared to the other characteristic fibroids (F). (B) After IV Gadolinium contrast administration, it shows homogeneous enhancement.

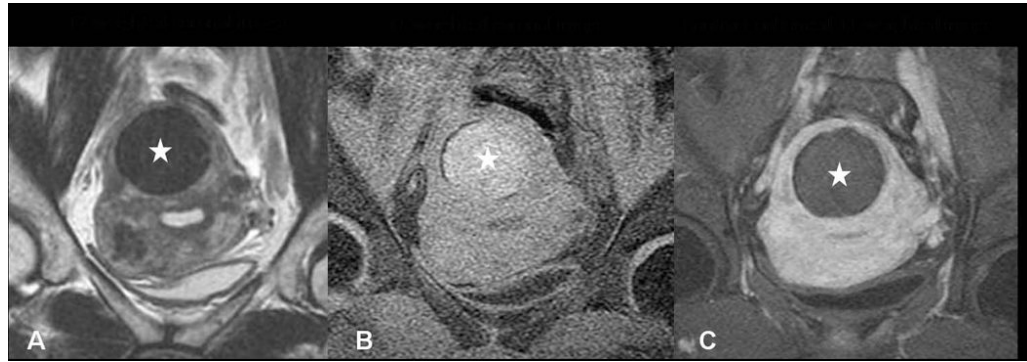


Figure 3. Degenerated fibroid, pretreatment screening MRI. The fibroid (stars in A, B and C) shows low signal intensity on T2 weighted imaging (A) and high intensity on T1 weighted imaging (B). (C) After IV Gadolinium contrast administration, it shows no enhancement.

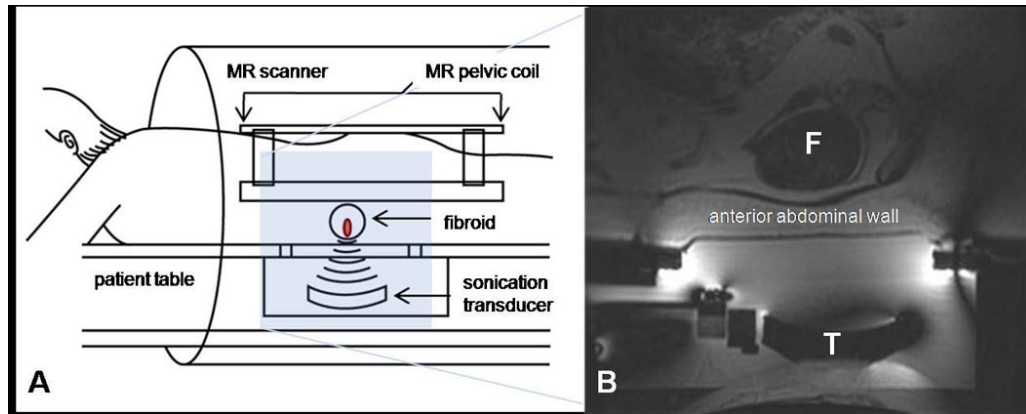


Figure 4. Overview of ExAblate 2000 device (InSightec Inc., Haifa, Israel). (A) treatment diagram of MRgFUS. The patient lies in a prone position on the treatment table that contains the transducer. The table is docked to the MR scanner. (B) sagittal MR image prior to treatment. F: fibroid, T: transducer. (Color version of figure is available online.)

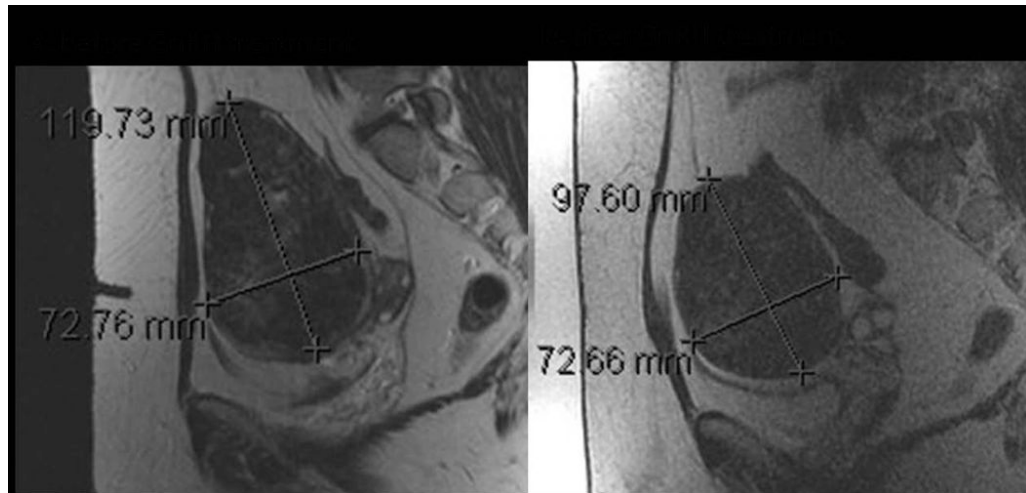


Figure 5. MR imaging of GnRH agonist effect. T2 weighted imaging of a large uterine fibroid, before (A) and three months after (B) treatment with GnRH agonist. The size of the fibroid is decreased, and the signal intensity has become homogeneously low after management.

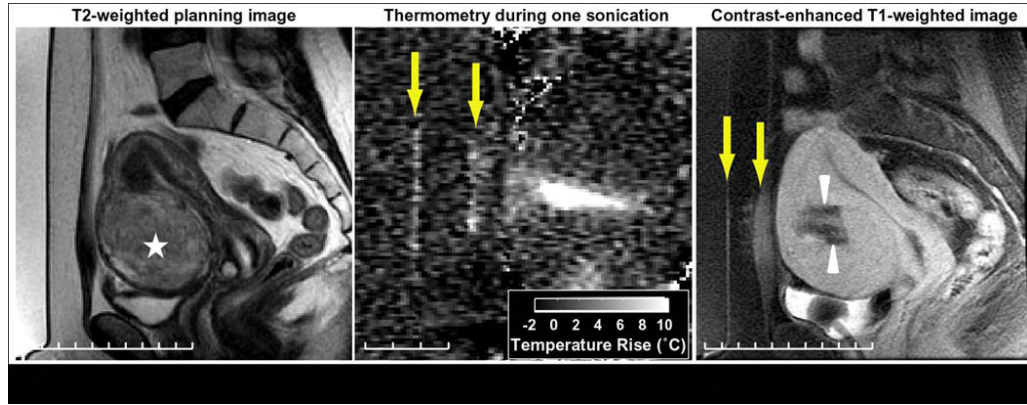


Figure 6. Challenging treatment of hypercellular fibroid and thermal damage outside of the fibroid. (A) On T2 weighted imaging, the hyperintensity of the target lesion (star) indicates that its hypercellular nature requires more energy to ablate it. (B) During treatment, low-level heating is visible in the muscle and skin (arrows) in the thermometry using the proton resonant frequency (PRF) shift technique. Heating is not observed in the fat because the PRF of lipids is not temperature-sensitive. (C) In the contrast-enhanced T1 weighted image performed immediately after treatment, enhancement at skin, subcutaneous fat, and muscle in front of the fibroid in the ultrasound beam path are noted (arrows), indicating thermal damage. This heating, along with skin pain, limited the maximum energy that could be employed and reduced the success of the treatment, which is evident by the sub-optimal non-perfused region (arrowheads). This was asymptomatic and these changes in the fat are no longer visible in the MR after six months.

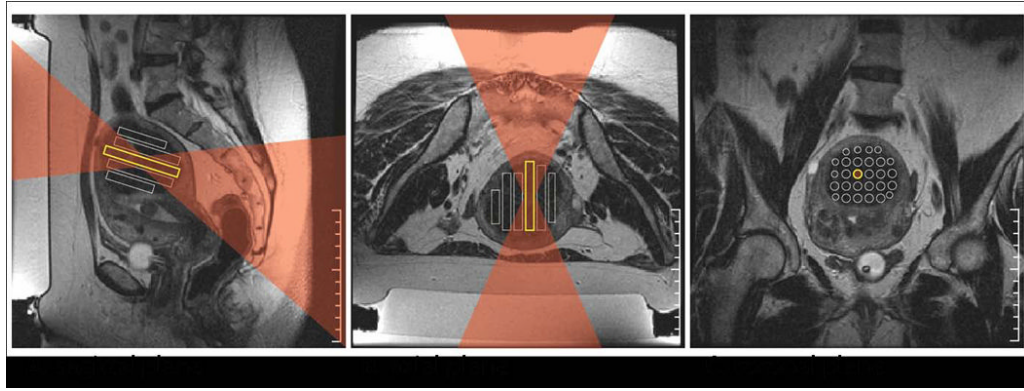


Figure 7.

Three-dimensional treatment planning for MRgFUS ablation of a uterine fibroid. On different planes of T2 weighted imaging, the operator defines the target locations and chooses the ultrasound parameters for locations and shape of the target lesion. (A) The ultrasound beam was angled to change the beam angle on the sacrum (S) and (C) the spacing between targets was found to be sparsely packed. (B) The axial plane shows the beam passage and planned sonications. For each location, the operator checks the ultrasound beam path (superimposed here in red) to ensure that it does not pass through any critical structures, such as bowel loops or scars. S: sacrum. (Color version of figure is available online.)

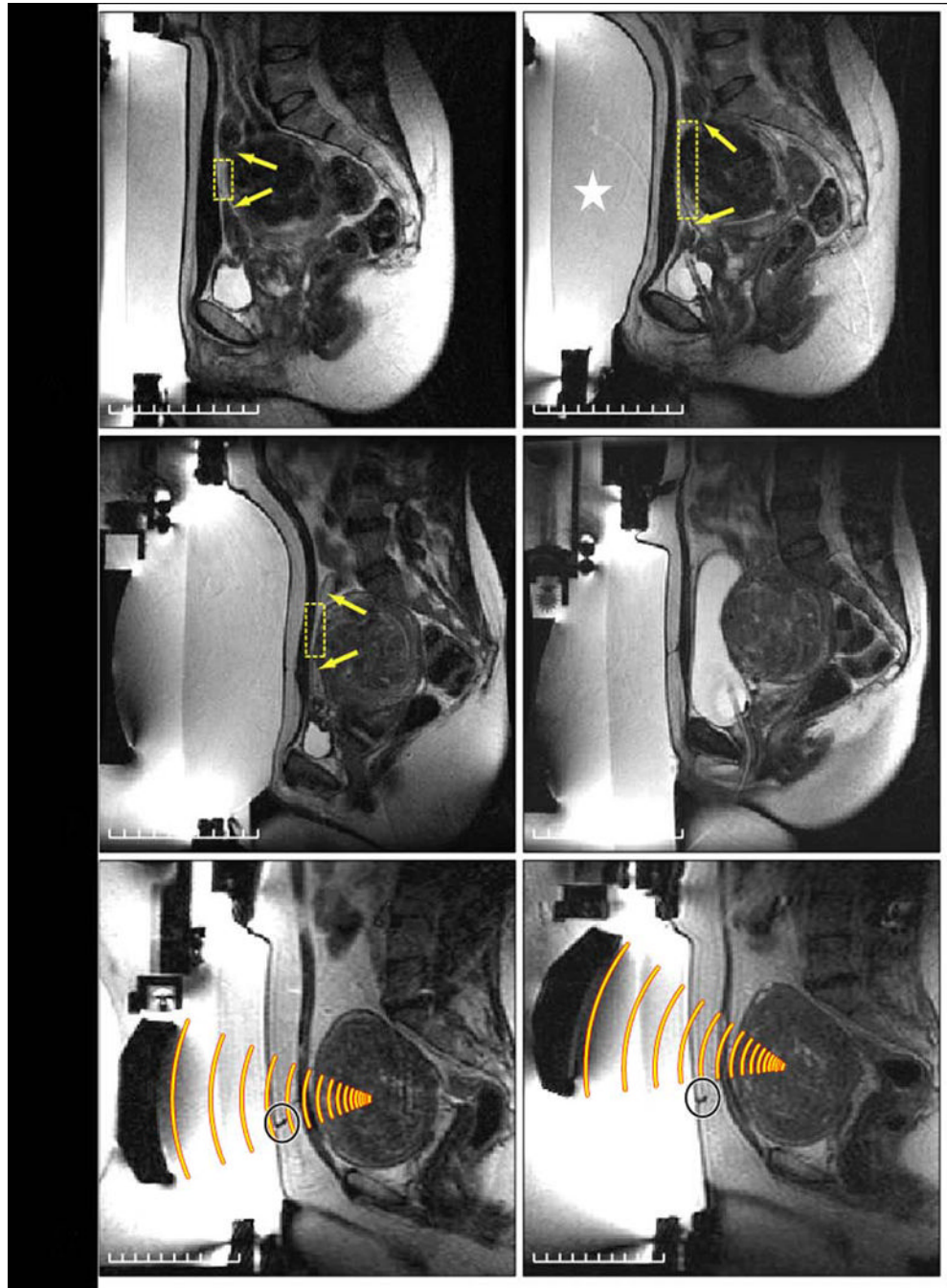


Figure 8.

Challenging treatment planning scenarios. (A) Left: In this patient, bowel loops are in front of the fibroid (arrows), thus initially reducing the size of the acoustic window (box). Right: To move these loops aside, a larger gel pad is placed below the abdomen (star), allowing access to most of the fibroid. (B) Left: In another patient, even with this larger gel pad, bowel loops are still in front of the fibroid (arrows), thus severely limiting the acoustic window (box). Right: To displace the loops further, normal saline is instilled into the urinary bladder via a Foley catheter, displacing the bowel loops superiorly and creating a wider acoustic window. (C) Left: The third patient has a scar directly in front of the fibroid (circle). Right: By tilting the ultrasound beam, the scar can be avoided. (Color version of figure is available online.)

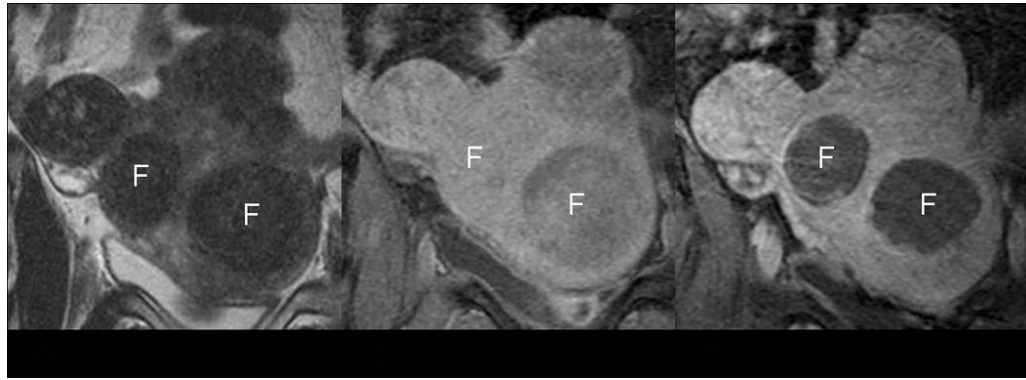


Figure 9.

Treatment effect in MR image. (A) On pretreatment T2-weighted coronal imaging, the uterine fibroids show homogeneously low signal intensity. (B) Before treatment, the fibroids show homogeneous enhancement after IV contrast administration. (C) After treatment, the contrast enhanced T1 weighted images revealed no enhancement in the fibroids, indicating complete necrosis. F: target fibroids.

Table 1

Suggested MRI protocol for imaging and characterization of fibroids

sequence	plane	slice thickness/interval (mm)	field of View (cm)
3 plane locator (single shot fast spine echo)	axial, coronal, sagittal	5, 0	30-36
T2 weighted fast spin-echo	axial, coronal, sagittal	4-5, 1-2	20-25
T1 weighted fat-suppressed spoiled gradient-echo	axial	4-5, 1-2	20-25
contrast-enhanced T1-weighted three-dimensional fat-suppressed spoiled gradient-echo	axial, coronal, sagittal		20-25

Table 2

The MR findings of fibroids

fibroid type	signal intensity on T1-weighted imaging	signal intensity on T2-weighted imaging	contrast enhancement pattern
classic	low	low	homogeneous
cellular	low	high	homogeneously strong
red (hemorrhagic) degeneration	high	low	none
necrotic degeneration	high	variable	none
cystic degeneration	high	low	none
myxoid degeneration	High	low	minimal
hyaline degeneration	variable	low	none
lipoleiomyoma	high	mixed	mixed

Table 3

The imaging findings need to be evaluated in the pre procedure MR and beam path planning

findings		treatment limitation	recommendation
size	too small (without dominant one) too large (> 10 cm)	poor treatment effect poor treatment effect	consider GnRH agonist treatment before MRgFUS
location	Too posterior (>12 cm from the center of the fibroid to abdominal wall or <4 cm to sacrum) Submucosal or subserosal (especially pedunculated) abdominal scar	limited US wave penetration, heating of sacrum and cause sciatic nerve injury	consider endoscopic treatment
acoustic window	intervening visceral organ (bladder or bowel)	may deviate US wave and cause skin burn visceral organ damage	angle the ultrasound beam to avoid passing through angle the ultrasound beam, displace the bowel with larger gel pad or by distending urinary bladder
fibroid character	degeneration (non-perfusion) hypercellular calcification	poor treatment effect poor treatment effect may interfere US propagation	